Proc. of the 2nd Int.Semiconductor Technology Conf. ISTC2002, Tokyo, Vol.2002-17(2002, ElectroCcemical Society)

PULSE DURATION EFFECTS ON LASER ANNEAL SHALLOW JUNCTION

A. Matsuno, K. Kagawa and Y. Niwatsukino
Research Center, Research Division, Komatsu Ltd.
1200 Manda, Hiratsuka, 254-8567 Japan, akira_matsuno@komatsu.co.jp

T. Nire
Phoeton Corp.
48-6 Teradanawa, Hiratsuka, 259-1215 Japan

K. Shibahara
**Research Center for Nanodevices and Systems, Hiroshima University
1-4-2 Kagamiyama, Higashi-Hiroshima, 739-8527 Japan

Ultra shallow junction was formed by KrF excimer laser anneal method changing laser pulse duration. A simple one-dimensional thermal diffusion model was utilized to obtain time dependent temperature profile and to understand the influence of the pulse duration on junction properties such as junction depth, sheet resistance and residual defects. The model analysis also suggested that substrate heating during laser irradiation was effective to reduce the required laser energy density to activate dopants by melting pre-amorphized layer.

INTRODUCTION

The scaling of Metal Oxide Semiconductor (MOS) integrated circuit has progressed below 100 nm of gate length. The short channel effects that source-drain current is controlled by drain space charge not by the gate voltage have been always the primary problem to be solved for the scaling steps. Ultra Shallow Junction (USJ) formation is one of the most fundamental and effective counter measures to suppress the short channel effects in MOSFETs. According to the International Technology Roadmap for Semiconductors 2001 Edition (ITRS 2001), the source/drain extensions with the junction depth of 13-22 nm and the sheet resistance lower than 770 Ω/sq. will be required in 2005 [1].

Rapid thermal annealing (RTA) with low energy ion implantation is the current standard to form USJ [2]. However, obtainable junction depth and sheet resistance with RTA will not match with the requirements for an 80 nm technology node. In case of RTA, wafer heat up time is order of seconds. Consequently, it is difficult to restrain the thermal diffusion of dopants, especially diffusion of boron. In addition, the sheet resistance is limited by the thermal equilibrium solid solubility of the dopant [3].

Various methods to form USJ has been reported as an alternative to RTA, for example, atomic layer doping [4], plasma doping [5], laser anneal [6, 7, 8] and so on. All of these methods have their own advantages and disadvantages. For example, the junction depth obtainable by the atomic layer doping method will satisfy the demands of a few coming generations, however, the sheet resistance is too high for practical applications. Laser annealing combined with low energy ion implantation has been reported as an effective method to achieve shallow junction depth and low sheet resistance at the same time. However the leakage current caused by residual defects [6] and difficulties in integrating to device fabrication process [3] still remain as problems for real production.

Previously it is pointed out by the authors that the sheet resistance and the junction depth were affected by laser pulse duration [8]. The laser pulse duration is important factor to modify the heating up and cooling down rate for the annealing. We have experimentally investigated the influence of the pulse duration more minutely. In addition, a one-dimensional thermal diffusion model calculation was utilized to understand the experimental results.

EXPERIMENTS

Si (100) wafers with a resistivity of 2–8 Ω·cm were prepared for the series of experiments. Boron ions were implanted into the Si wafers after germanium implantation for pre-amorphization. The energy and the dose of the boron implantation were 0.5 keV and $5x10^{14}$ cm^{-2}, respectively. Afterwards, the Si wafers were irradiated with KrF (248 nm) excimer laser beams whose pulse durations were 10 ns, 38 ns and 62 ns. Figure 1 shows transient waveform of these laser pulses. Boron depth profiles were measured by Secondary Ion Mass Spectrometry (SIMS) and the sheet resistance were measured by a two-point prove method. Cross sectional Transmission Electron Microscopy (TEM) was used to observe the defects in the wafers.

RESULTS AND DISCUSSION

Experimental results

Figure 2 shows the typical boron SIMS depth profiles for as implanted and laser annealed specimens. The laser pulse duration for Fig. 2 was 38 ns. The junction depth was defined as the depth at which the boron concentration was $1x10^{18}$ cm^{-3}. In the case of laser annealing with melting process, the junction depth is mainly determined by the melting depth because of large difference in the boron diffusion coefficients in solid and liquid phase. In the case of submelt, that is, the laser annealing without melting process, the junction depth is almost same as the ion implantation range, as shown in Fig. 2 for 500 mJ/cm^2. Box like profiles were obtained for the laser energy densities of 600 mJ/cm^2, 700 mJ/cm^2 and 800 mJ/cm^2. In these profiles, plateau regions can be seen and the width is considered to be nearly equal to the malting depth. The annealing process of the irradiated area is classified to the following three states in term of the melting, (I) submelt, (II) pre-amorphized layer melts (about 20 nm of junction depth) and (III) pre-amorphized layer and crystalline Si substrate melt. It is noticeable in Fig. 2 that the state (II) appears for a certain energy density range. The width of the energy density range is attributed to the melting point difference between a-Si and c-Si [9]. The same classification can be applied also to other pulse durations.

Figure 3 shows the junction depths obtained with SIMS depth profiles as a function of laser energy density for the three pulse durations. The junction depth becomes deeper as the laser pulse duration becomes shorter even for the same laser energy density. The threshold energy to melt the Si surface increases as the pulse duration became longer. For example, about 400 mJ/cm^2 to 500 mJ/cm^2 of the energy density was required to melt the pre-amorphized layer with the10 ns laser pulse. On the other hand, more than 700 mJ/cm^2 was required for the 62 ns pulse.

The sheet resistance is also affected by the pulse width. As shown in Fig. 4, the sheet resistance once decreases and then saturates as the laser energy density is increased. It is noted that, in the cases of 10 ns and 38 ns pulse widths, the decrease in the sheet resistance by increasing the energy density is seen in the state (II) in which the junction depth was about 20 nm and constant independent of the laser energy density. Under such condition, the sheet resistance for 38 ns was lower than that for 10 ns. In the case of 62 ns, the laser energy density was too small to achieve a low enough sheet resistance to the extent of our experiments. The obtained best combination of the sheet resistance and the junction depth was 490 Ω/sq. and 20 nm, respectively in the case of 38 ns laser anneal for the laser energy density of 700 mJ/cm^2. These values meet the requirement of the 80 nm node in ITRS2001.

Figure 5, 6 and 7 show the cross sectional TEM images for as implanted (Fig. 5) and after the annealing with 10 ns (Fig. 6) and 38 ns (Fig. 7) laser beam. The laser energy densities were both 600 mJ/cm^2. The energy density leads to the state (II) for 38 ns pulse. Pre-amorphized layer whose thickness is about 12 nm is seen in Fig. 5. In Fig. 7, high-density twins [8] are observed underneath the silicon surface. Their depth is almost same as that for the pre-amorphized layer. This implies that the twin was originated from the interface between amorphous and crystal phases. On the other hand, in Fig. 6, a number of smaller defects can be seen but twins. These facts suggest that the crystallinity for the 38 ns laser beam was better than that for the 10 ns laser beam as long as the state (II).

Simulation of heat flow

A simple one-dimensional thermal diffusion model calculation was utilized to explain these experimental results from the viewpoint of heat flow. The followings are thermal diffusion equations with the term of laser heating.

$$c\rho\frac{\partial T}{\partial t}=\frac{\partial}{\partial x}\left(k\frac{\partial T}{\partial x}\right)+\alpha(1-R)I(x,t) \quad (1)$$

$$\frac{\partial T}{\partial x}=0 \quad (x=0) \quad (2)$$

$$T=T_{sub} \quad (x=L) \quad (3)$$

where c: specific heat, ρ: density, k: thermal conductivity, α: absorption coefficient, R: reflectivity, and I(x,t): laser power. The boundary conditions are given by equations (2) and (3). The

Table 1 Parameters used in this work

	crystal	amorphos	liquid
c (J/g K)	0.707	0.707	0.707
ρ (g/cm^3)	2.33	2.33	2.33
k (W/cm K)	0.235+4.45exp(-T(K)/247)	0.235+4.45exp(-T(K)/247)	0.67
Latent Heat (J/g)	1800	1250	-
α (cm^{-1})	$2x10^6$	$2x10^6$	$2x10^6$
R	0.68	0.68	0.7
m.p.(K)	1687	1387	-

left-hand side of equation (1) stands for the enthalpy variation. The boundary condition of the surface that is irradiated by laser beam was assumed to be heat insulation and the bottom was assumed to be constant temperature, that is, the substrate temperature.

The dependence of k on temperature and R on phases were considered. Other parameters were treated as constants. The phase transition between solid and liquid were treated by enthalpy-based method. The melting point of the surface 15 nm that corresponds to the pre-amorphized layer was assumed to be lower than crystalline Si by 300 ^{o}C. The parameters values are summerized in table 1 [10].

The laser pulses were assumed triangular, as shown in Fig. 8, whose rise time is 5 ns, and pulse widths (defined by full-width at half maximum (FWHM)) were modified to simulate the experimental by changing its fall time. The effect of substrate temperature was also considered. The differential equation was transformed into finite difference equation and solved by the finite differnce method. The numerical solusion was based on the impricit method. The thermal conductivity between two elements was put harmonic avarage of the thermal conductivity of both two elements because of their temperature dependence.

Figure 8 shows a calculation resuls of the temporal temperature variation for each depth with the illustration of the laser pulse in same time scale. The laser pulse used for the the calculation was 5 ns of rise time, 35 ns of FWHM and 875 mJ/cm^2 of energy density. Concerning fromthe surface to 44 nm in depth, the temperature for every 2 nm is plootted. We can see that the surface pre-amorphized layer melts at the temperature of a-Si melting point (A) and the crystalline Si substrate melts at the temperature of c-Si melting point (B) in Fig. 8. Both melts solidifys at the temperature of c-Si melting point (C). The melting region and the solidificating region can be identified as the constant temperature region because of the latent heat. The melt depth was defined as the maximum depth where peak temperature exceeds the melting point. The solidification time was defined as the time difference between the timings for cooling down to the meltimg point at the melt bottom and the surface. Then the solidification velocity was obtained by deividing the melt depth by the solidification time. In the case of Fig. 8, the calculated melt depth and the solidification velocity are 36.5 nm (15 nm of pre-amorphized Si and 11.5 nm of Si substrate) and 1.7 m/s, respectively.

Figure 9 shows the calculated melting depth of Si as a function of the laser energy density.

The plateaus where the calculated melt depth is limited by the pre-amorphized depth for a certain energy density range are clearly seen in this figure. As described with the experimental results in Fig. 3, the plateaus are attributed to the difference in the melting point between pre-amorphized Si and c-Si. In other words, this region corresponds to the state (II) in Fig. 3. The tendency that a higher energy density is required to melt the pre-amorphized Si layer as the laser pulse duration increase is also confirmed by this calculation. Thus, simulated result well agrees with the experimental results in Fig. 3.

Figure 10 shows the calculated solidification velocity as functions of laser energy density for the three pulse durations. According to Fig. 10, the solidification velocity varies even in the plateau region shown in Fig. 9. In the plateau region, the solidification velocity becomes slow as the laser energy density increases. The solidification velocity has the minimum at the highest energy density point of the plateau region. The laser pulse duration affects the solidification velocity. As the laser pulse duration becomes longer, the minimum solidification velocity for each pulse duration becomes slower. In general, it is considered that too fast solidification velocity gives rise to disordering in lattice, that is, residual defects. It has been reported that the maximum solidification velocity that obtains re-crystallization without a-Si is 15 m/s [10]. The solidification velocity for the 10 ns pulse in Fig. 10 is close to this value. This coincides the residual amorphous layer observed in the TEM image in Fig. 6. Even if the solidification velocity is much smaller than 15 m/s, lower solidification velocity is preferred in terms of defect density as shown in Fig. 7 and higher activation or lower sheet resistance as shown in Fig. 4.

Figure 11 shows the effect of the substrate temperature on the melt depth. The laser pulse duration was assumed to be 35 ns. It should be noted that the required laser energy to melt the pre-amorphized Si layer for 723 K of the substrate temperature was about half of that for 300 K. Figure 12 shows the solidification velocity as a function of laser energy density for the same condition as Fig. 11. The minimum solidification velocity is slightly reduced by the substrate temperature increase. Therefore, nearly equal or slightly improved defect density and sheet resistance is expected by heating the substrate with much reduced laser energy densities. The laser energy reduction can be utilized to improve throughput by enlarging the exposure area or reducing equipment cost for the same exposure area with low power laser source.

SUMMARY

The laser anneal method to form the ultra shallow junction has been investigated experimentally and theoretically. The laser pulse duration affected the junction properties, such as junction depth, sheet resistance and crystal defect density. The results of simple one-dimensional thermal diffusion simulation qualitatively agree with the experimental results. The calculated solidification velocity can explain the experimental results of the sheet resistance and crystal defects. The effect of substrate temperature shows the possibility to reduce the laser energy density to activate dopants.

ACKNOWLEDGEMENTS

The authors wish to thank A. Mineji for measuring SIMS profiles and sheet resistance of the junctions. This work was partly supported by NEDO/MIRAI Project.

REFERENCE

[1] International Technology Roadmap for Semiconductors 2001.

[2] T. Matsuda, S. Shishiguchi and H. Kitajima., Extended Abstract of the first International Workshop on Junction Technology, 29 (2000).

[3] S. Talwar, Y. Wang and C. Gelatos, *Electrochem. Soc. Symp. Proc.*, 2000-9 95 (2000)

[4] M. Koyanagi, Extended Abstract of the first International Workshop on Junction Technology, 1 (2000).

[5] R. B. Liebelt, S. R. Walther, S. B. Felch, Z. Fang, B. -W. Koo and D. Hacker, Extended Abstract of the first International Workshop on Junction Technology, 23 (2000).

[6] K. Goto, T. Yamamoto, T. Kubo, M. Kase, Y. Wang, T. Lin, S. Talwar and T. Sugii, IEDM-99, IEEE, (1999), 931

[7] B. Yu, Y. Wang, H. Wang, Q, Xiang, C. Riccobene, S. Talwar and M. -R. Lin, IEDM-99, IEEE, (1999), 348

[8] K. Kagawa, Y. Niwatsukino, A. Matsuno and T. Nire, Extended Abstract of the second International Workshop on Junction Technology, 99 (2001).

[9] Y. Yonezawa and T. Minamikawa, *Report of the Industrial Research Institute of Ishikawa*., 48 (1999)

[10] A G Cullis, *Rep. Prog. Phys.*, **48**, 1155 (1985)

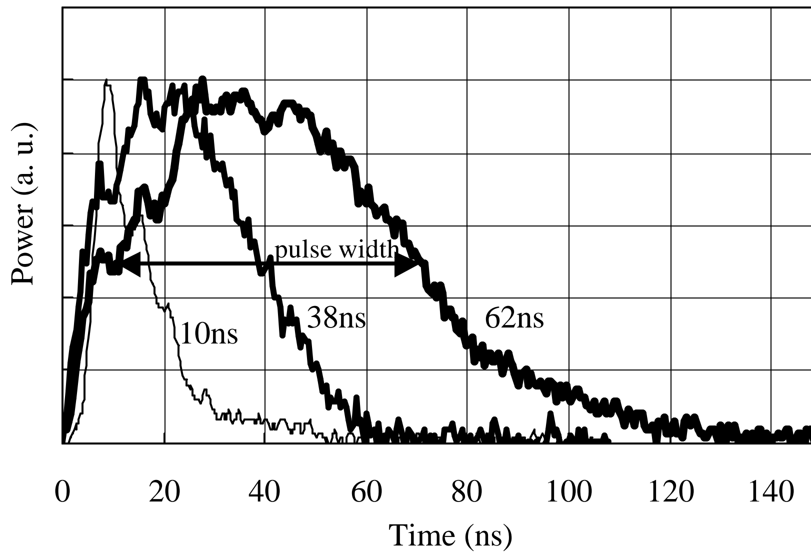

Fig. 1 Transient waveforms of the laser beams used in this work.

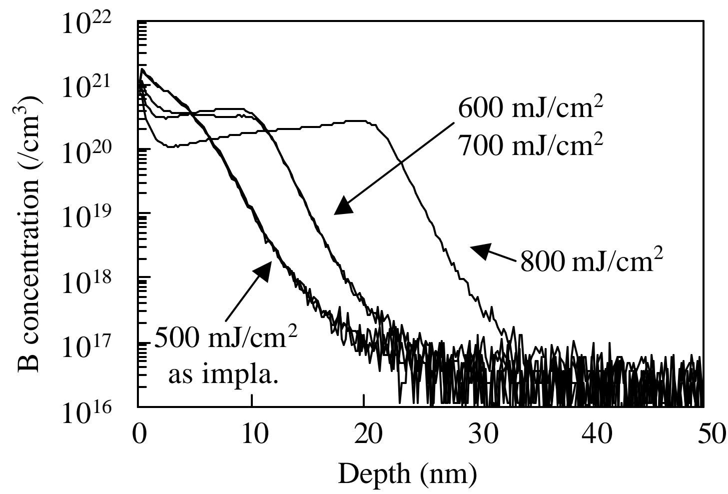

Fig. 2 Boron depth profile annealed by 38 ns pulse duration laser measured by SIMS.

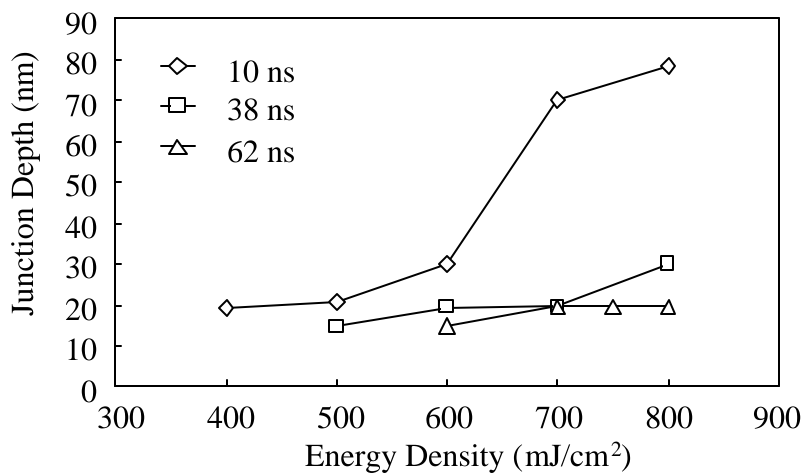

Fig. 3 Junction depths obtained with SIMS depth profiles as a function of laser energy density (experimental results).

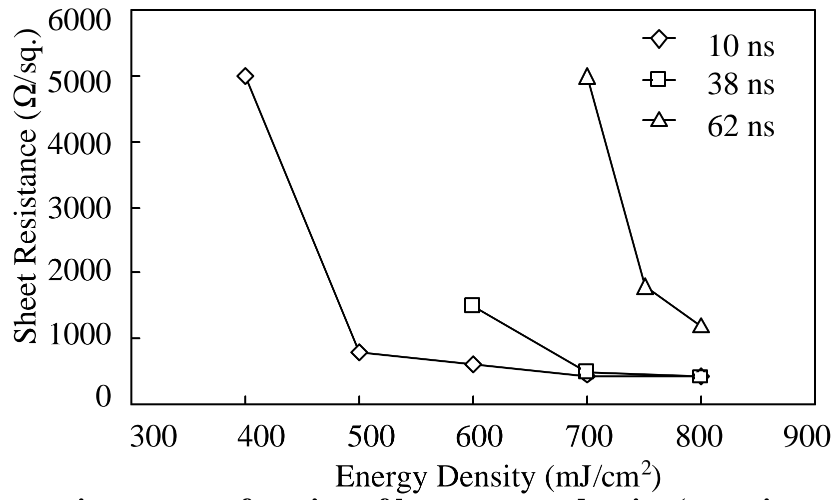

Fig. 4 Sheet resistance as a function of laser energy density (experimental results).

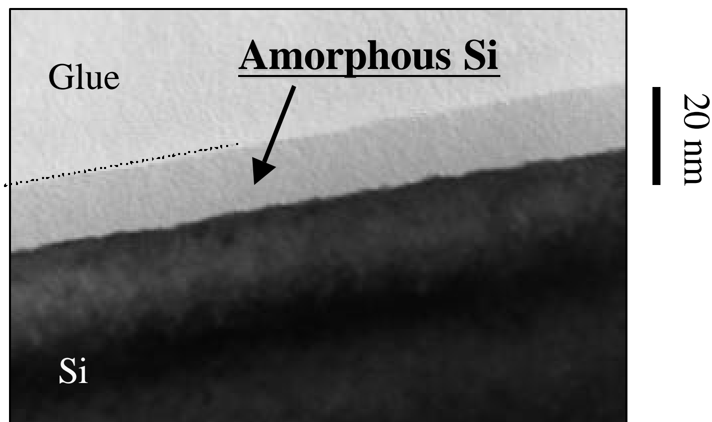

Fig. 5 Cross sectional TEM image of as implanted Si wafer.

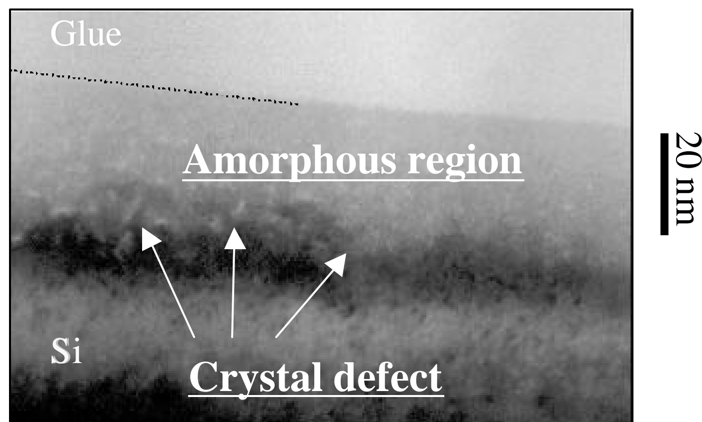

Fig. 6 Cross sectional TEM image after the annealing with 10 ns pulse duration.

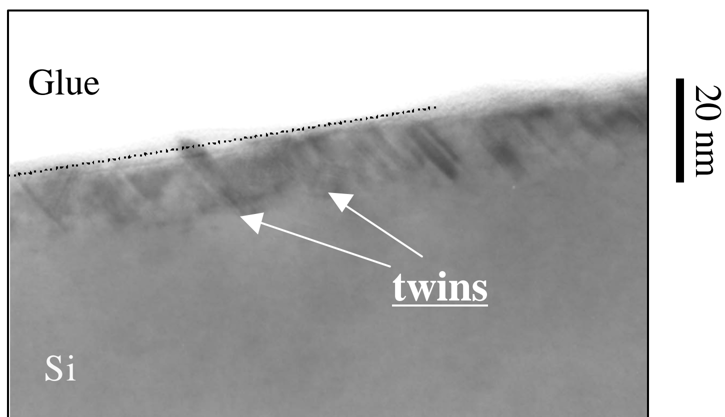

Fig. 7 Cross sectional TEM image after the annealing with 38 ns pulse duration.

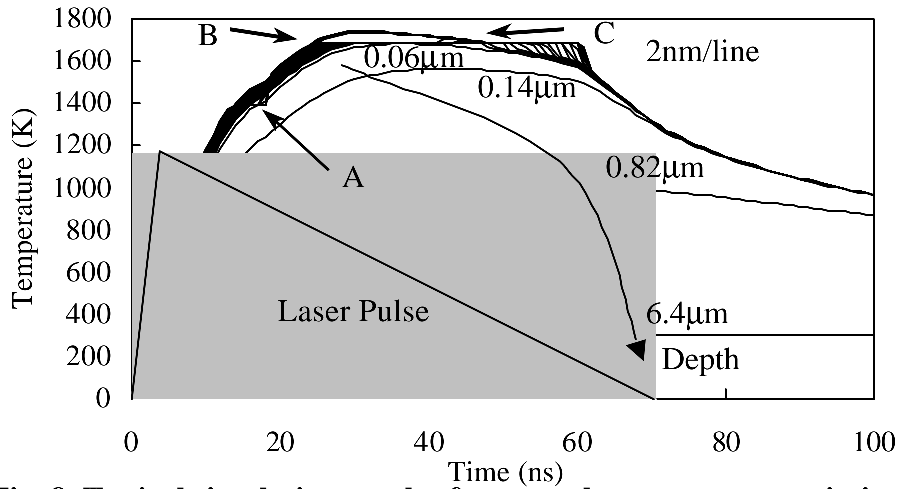

Fig. 8 Typical simulation result of temporal temperature variation for each depth. The values in the figure stand for the depth form the surface. The curves near the values are the temporal temperature variation at the depth explained by the values. The step of the depth near surface shown in the figure is 2 nm/line and it is too small to explain in the figure directly. A: a-Si melting, B: c-Si melting, C: Si solidification

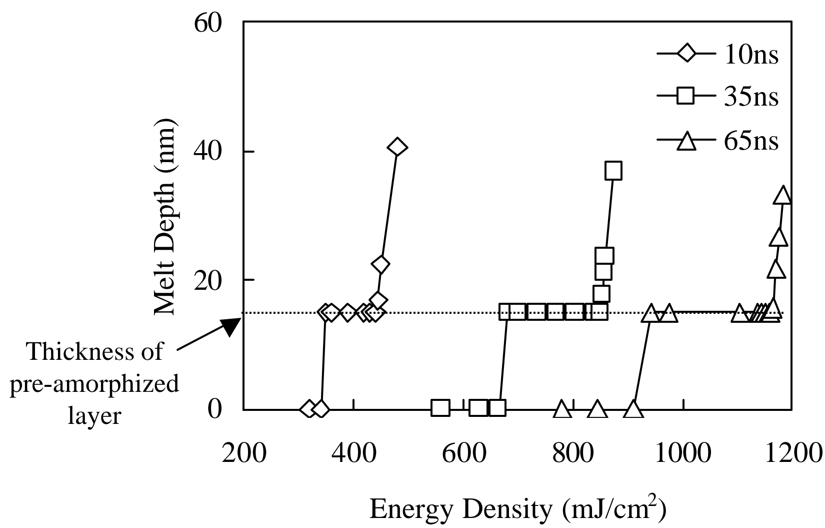

Fig. 9 Melt depth vs. laser energy density for each pulse duration (calculation results).

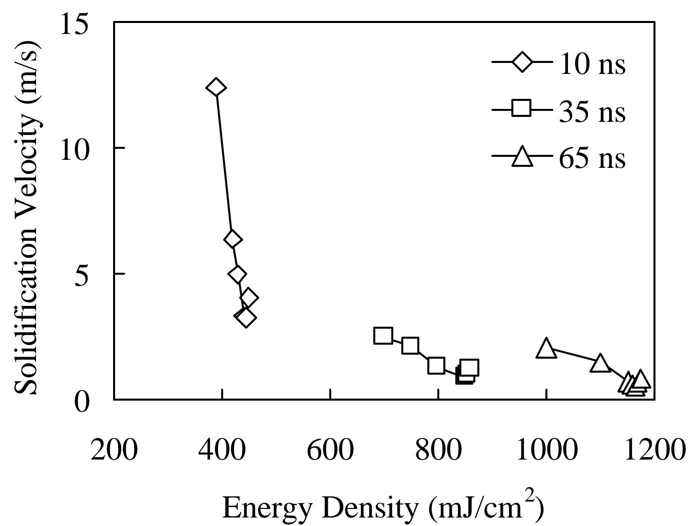

Fig. 10 Solidification velocity vs. laser energy density for each pulse duration (calculation results).

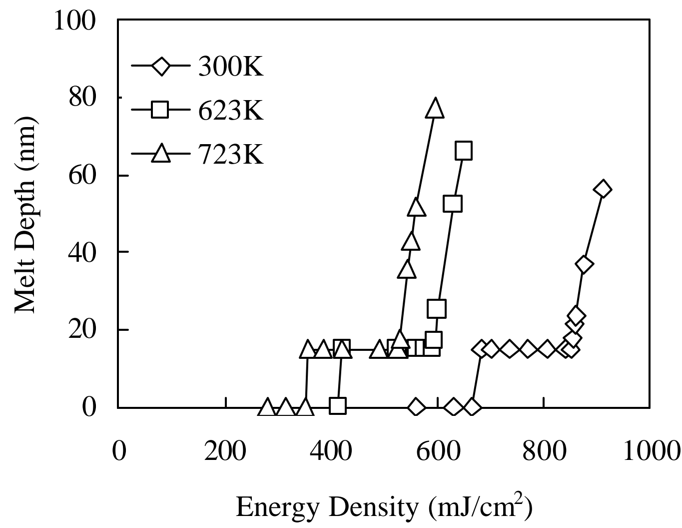

Fig. 11 Melt depth vs. laser energy density for each substrate temperature (calculation results).

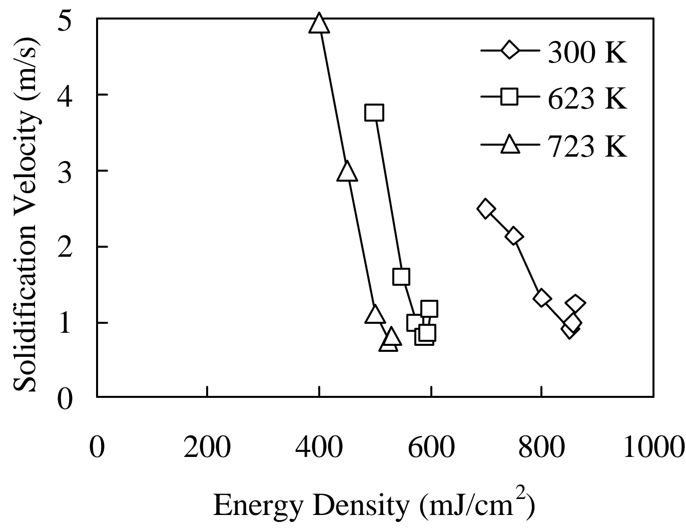

Fig. 12 Solidification velocity vs. laser energy density for each substrate temperature (calculation results).